LAWRENCE
LIVERMORE
NATIONAL
LABORATORY

LLNL-JRNL-644153

Root Exudates Counteract Mineral Control on Soil Carbon Turnover

M. Keiluweit, J. Bougoure, J. Pett-Ridge, P. K. Weber, P. S. Nico, M. Kleber

September 23, 2013

Nature Climate Change

Disclaimer

Mineral Protection of Soil Carbon Counteracted by Root Exudates

Marco Keiluweit[1,2], Jeremy J. Bougoure[2,3], Peter S. Nico[4], Jennifer Pett-Ridge[2], Peter K. Weber[2] and Markus Kleber[1,5]*

[1] Department of Crop and Soil Science, Oregon State University, ALS Building 3017, Corvallis, OR-97331, USA

[2] Chemical Sciences Division, Lawrence Livermore National Laboratory, 7000 East Ave, L-231, Livermore, CA-94550, USA

[3] School of Earth & Environment, University of Western Australia, 35 Stirling Hwy, Crawley. 6009, Australia

[4] Earth Sciences Division, Lawrence Berkeley National Laboratory, 1 Cyclotron Rd, Berkeley, CA-94720, USA

[5] Leibnitz-Zentrum fur Agrarlandschaftsforschung (ZALF) e.V. Eberswalder Straβe 84, 15374 Müncheberg, Germany

[*]Corresponding author address:

Marco Keilweit

Stockbridge School of Agriculture

University of Massachusetts—Amherst

411 Paige Laboratory

Amherst, MA-01003, USA

Email: keiluweit@umass.edu

Abstract

Multiple lines of existing evidence suggest that climate change enhances root exudation of organic compounds into soils. Recent experimental studies show that increased exudate inputs may cause a net loss of soil carbon (C). This stimulation of microbial carbon mineralization ('priming') is commonly rationalized by the assumption that exudates provide a readily bioavailable supply of energy for the decomposition of native soil C (co-metabolism). Here we show that an alternate mechanism can cause C loss of equal or greater magnitude. We find that a common root exudate, oxalic acid, promotes carbon loss by liberating organic compounds from protective associations with minerals. By enhancing microbial access to previously mineral-protected compounds, this indirect mechanism accelerated carbon loss more than simply increasing the supply of energetically more favorable substrates. Our results provide novel insights into the coupled biotic-abiotic mechanisms underlying the 'priming' phenomenon and challenge the assumption that mineral-associated carbon is protected from microbial cycling over millennial time scales.

Introduction

Plants direct between 40-60% of photosynthetically fixed carbon (C) to roots and associated microorganisms via sloughed-off root cells, tissues, mucilage and a variety of exuded organic compounds [1,2]. Elevated CO_2 concentrations in the atmosphere are projected to increase the quantity [3,4] and alter the composition [5,6] of root exudates released into the soil. It seems less clear to what extent changing inputs will cause a net loss of native (or 'old') organic C [7]. A better understanding of the mechanism underlying soil C loss is pivotal in predicting how the large soil C stocks may respond to global change.

Exudate-induced soil C loss is commonly attributed to a 'priming effect', i.e. a short-term increase in microbial mineralization of native soil C as a result of fresh carbon inputs to the soil [8]. Although the process of 'priming' has received great attention in ecosystem sciences in recent years [8,9], our knowledge of the underlying mechanism is limited. It is often supposed that bioavailable exudate compounds induce greater microbial activity and enzyme production because they serve as 'co-metabolites' [8,10]. Co-metabolism is defined as the mineralization of a non-growth substrate (e.g., certain forms of native soil organic C) during growth of a microorganism on a bioavailable carbon and energy source (e.g., exudate compounds) [11]. This mechanism is often invoked to increase the physiological potential of decomposers for the mineralization of native soil C [8,10] (Fig. 1a). However, as noted by Kuzyakov and co-workers [12], direct experimental evidence in support of this mechanism is scarce because most studies have aimed at identifying 'priming effects' rather than the underlying mechanism.

Previous attempts to describe the mechanism(s) underlying 'priming effects', have focused almost exclusively on biological phenomena. That approach, however, results in a conceptual conundrum: How can observed 'priming effects' be explained solely by co-metabolism if microbial access to substrate C is notoriously limited in most soils? In mineral soil, the majority of organic

compounds is intimately associated with reactive mineral phases [13,14]. Metal-organic complex (MOC) and short-range order (SRO) phases bind organic compounds through their large surface area and various bonding sites [15,16]. Such mineral-organic associations limit microbial and enzymatic access [17] and are quantitatively the most important mechanism protecting C from microbial use for centuries or millennia [18]. Rasmussen et al. [19] showed that the magnitude of the 'priming effect' is at least partly controlled by the presence of reactive mineral phases. Recent conceptual frameworks [20,21] and numerical models [22] therefore argue that C mineralization rates are generally enhanced by mechanisms that facilitate the release of mineral-protected C into more accessible pools.

Here we tested whether the acceleration of carbon mineralization in the rhizosphere (i.e., the priming effect) is promoted by the exudates' ability to liberate C from protective mineral-organic associations, thereby increasing microbial access. In a well-controlled system, we investigated the effects of the two most abundant exudate classes – organic acids and simple sugars [23,24]. We hypothesized that direct dissolution of protective mineral phases would be promoted by oxalic acid (Fig. 1b). Oxalic acid – an organic acid produced by roots, root-associated fungi and bacteria – is routinely found among the most abundant compounds in rhizosphere pore water [23,24]. Oxalic acid has strong metal complexing abilities but is of limited bioenergetic use to microbes. In contrast, we expected bioenergetically more favorable sugars such as glucose to act as a co-metabolite and stimulate microbial mineralization of native soil C (Fig. 1a). A third common exudate, acetic acid, was expected to have an intermediate response, as it is less easily metabolized than glucose and has a lower complexing capacity than oxalic acid (Table 1).

Recreating a rhizosphere environment

We tested these hypotheses by delivering a continuous supply of individual exudate solutions through an artificial root (length = 10 cm, diameter = 2.5 mm) into unperturbed soil, recreating a rhizosphere environment (Fig. S-1). Exudates were supplied to a grassland soil (Table S-1) at root surface-normalized rates mimicking natural exudation rates of root tips (15 μmol C cm^{-2} d^{-1}) [25,26]. For comparison, selected analyses were conducted on a forest soil. To distinguish exudate C from native soil C, individual exudate solutions were isotopically labeled with ^{13}C ($\delta^{13}C$ = 8800 ‰). Exudate solutions or an inorganic nutrient solution (control) were provided over a 35-d incubation period to replicate a burst in root growth at the onset of the growing season when the highest exudation rates are expected [26]. Compared to the control, all three exudate compounds induced visible physical gradients surrounding the artificial root after 7-10 days, which remained stable until the end of the experiment. In the oxalic acid treatment, these pronounced effects developed around the entire root and extended up to 5-10 mm into the soil (Fig. 2a), but in soils receiving glucose and acetic acid additions were limited to small patches around the root.

If root exudates accelerate the microbial mineralization of soil C (i.e., cause 'priming effects') primarily because they serve as a co-metabolite (i.e., provide easily assimilable C and energy) (Fig. 1a), one would expect energetically favorable glucose to cause a greater 'priming effect' than less favorable substrates such as oxalic acid (Table 1). However, we found that oxalic acid additions led to greater microbial respiration, community shifts to fast growing, rapidly C-mineralizing microbial taxa, and less soil C overall relative to the other treatments. This accelerated microbial C mineralization caused by oxalic acid exudates coincided with the disruption of mineral-organic associations and increases in C accessibility in the pore water. The following describes evidence that this 'priming effect' is at least in part caused by the exudates' ability to enhance microbial access to previously protected soil C (Fig. 1b).

Oxalic acid accelerated microbial carbon mineralization (i.e., 'priming effects') in the rhizosphere

To determine the effect of root exudates on microbial respiration rates in rhizosphere microsites, we used microsensors to record O_2 profiles in the soil surrounding the root (Fig. 2b). These profiles showed that addition of oxalic acid significantly depleted O_2 availability up to 5 mm into the surrounding soil ($p < 0.05$) (Fig. 2b), while the effect of glucose and acetic acid additions was restricted to the first 1.5 mm. Across the entire rhizosphere zone (0-15 mm), microbial respiration rates followed a consistent pattern: oxalic acid > glucose > acetic acid (Fig. 2b, inset). To test whether this was a response specific to the grassland soil (silt-loam), we repeated the experiment with a forest soil (clay-loam) differing in texture and mineralogy (Table S-1) and observed the same result (Fig. S-1). Overall, microbial respiration in the oxalic acid treatment exceeded that of glucose by a factor of ~1.6 (silt-loam) and ~2.8 (clay) (Table 1).

We compared the stoichiometry of microbial carbon-use efficiency (CUE) and biochemical oxygen demand (BOD) of oxalic acid versus glucose mineralization pathways and found that oxalic acid addition accelerated the mineralization of native soil C more than glucose addition. Reported CUEs (the ratio of C assimilated into new biomass relative to the amount of C used in cellular respiration) for oxalic acid (5-25%) and glucose (40-70%) in soils [27–29] indicate that the fraction of oxalic acid C released as CO_2 (75-95%) is about twice that of glucose C (30-60%). Mineralization (i.e., complete oxidation) of oxalic acid to CO_2 requires 0.25 moles of O_2 per unit C compared to 1 mole of O_2 per unit C for glucose (Table 1). The BOD expected for the mineralization of each substrate is equal to:

$$\text{Expected BOD} = (1 - \text{CUE}) \times \text{stoichiometric BOD} \qquad \text{equation (1)}$$

The CUE and stoichiometric BOD values used are shown in Table 1. These calculations demonstrate that the BOD expected for microbial mineralization of oxalic acid should only be half the value associated with glucose mineralization (Table 1). Because our measured respiration rates show the opposite trend, we conclude that mineralization of other, more reduced (non-exudate) soil C must have accounted for at least 50% of the respiration observed in the oxalate treatment.

In line with accelerated mineralization of native soil C, soils receiving oxalic acid additions experienced a net C loss in the zone closest to the root ($p < 0.05$) (Fig 3a). In contrast, addition of the energetically more favorable substrates glucose and acetic acid resulted in a pronounced increase in total soil C content (Fig. 3a). This net C accumulation, likely due to an increase in microbial biomass C caused by microbial assimilation of these exudates, was not counterbalanced by concurrent increases in the mineralization of native C.

Pronounced compositional changes in microbial community structure also reflect greater carbon mineralization activity in soil receiving oxalic acid (Fig. S-3a). Near the root (0-4 mm), oxalic acid additions significantly increased the relative abundance of Bacteroides and Proteobacteria and reduced that of Acidobacteria, Firmicutes and Verrucomicrobia ($p < 0.05$) (Fig. S-3b). Microbial communities in acetic acid amended soils shifted in a similar but less pronounced manner relative to oxalic acid treated soils; glucose had very little effect. Taxa from the Bacteroidetes and Proteobacteria phyla that were strongly promoted by the oxalic acid treatment, are often characterized as copiotrophs, and positively correlated with increased C bioavailability and mineralization rates [30,31].

Excess dissolved CO_2 measured in the pore water provides further evidence for accelerated C mineralization in the oxalic acid treatment. Measured immediately after harvest, the pH of soil close to the root was 1.5 and 0.7 units higher in oxalic and acetic acid treatments, respectively, while glucose lowered the pH by 0.5 units (Table S-6). This increased proton

consumption can be attributed to one or a combination of factors, all of which are linked to increased microbial activity: microbial decarboxylation [32], mineral dissolution reactions [33], dissimilatory metal reduction [34] and/or denitrification [35]. More importantly, however, we observed further pH increases in the oxalic acid treatment when samples were allowed to equilibrate with the atmosphere. This observation suggests that removal of excess dissolved CO_2, produced by microbial mineralization over the course of the incubation, diminished the buffering capacity of the soil.

In summary, we find that oxalic acid additions accelerate microbial C mineralization and lead to a significant loss of native C (~4%), consistent with previous observations of strong 'priming effects' induced by oxalic acid [36,37].

Spectroscopic insights into the 'priming' mechanism

To test whether disruptions of protective mineral-organic associations are responsible for the 'priming effect' we observed, sequential extractions targeting metal-organic complexes (MOC) and short-range order (SRO) phases were performed (Fig. 3b). Compared to the control, oxalic acid addition significantly decreased concentrations of Fe and Al phases up to 12 mm into the soil ($p < 0.05$). Specifically, Fe and Al in MOCs decreased with increasing proximity to the root, paralleled by a notable decline of Fe in SRO phases. Acetic acid exudates also significantly reduced the amount of Fe and Al in MOCs in the zone closest to the root ($p < 0.05$), while glucose showed no measureable effect. There were no significant responses of more crystalline pools to the exudate treatments. Complimentary batch experiments showed that oxalic acid caused greater mobilization of Fe and Al after short a short incubation of 1 hour than after a prolonged incubation period (48 h) (Table S-10); glucose showed no such effect. We infer that in our system, physiological levels of oxalic acid disrupt mineral-organic associations via an immediate, abiotic mechanism rather than slower,

180 microbially-mediated processes. This mechanism is more effective for mineral-organic associations
181 formed by amorphous MOCs than more crystalline SRO phases, a result consistent with
182 observations of stronger 'priming effects' (i.e., accelerated mineralization of native soil C) in soils
183 dominated by amorphous MOCs than in soils characterized by more crystalline Fe oxides phases [19].

184 We further examined the concentration and speciation of pore water C and metals as a test
185 for the liberation of mineral-bound organic C (Table S-6). In the near-root zone (0-4 mm), oxalic
186 acid addition increased pore water C concentrations by a factor of ~8 compared to the control,
187 while acetic acid and glucose additions affected C concentrations only by factors of ~2.5 and ~1,
188 respectively. This increase in dissolved C in the pore water correlated with increases in dissolved
189 Fe (R^2 = 0.98) and Al (R^2 = 0.95) (Fig. 4a, Table S-6). The bulk chemical composition of organic C in
190 the pore water was determined by laser desorption post ionization mass spectrometry (LDPI-MS), a
191 method that is particularly sensitive for lignin-derived compounds [38]. Mass spectra of pore water
192 from the oxalic acid treatment showed a notably greater abundance of high mass-to-charge peaks
193 (m/z = 250 to 500) relative to the other treatments (Fig. S-4). These mass peaks can be attributed
194 to aromatic dimers based on the relatively low ionization energy of aromatic compounds [39] and
195 peak patterns resembling those of lignin in soils [38]. These results support the hypothesis that oxalic
196 acid addition chemically disrupted MOCs and SRO mineral phases in the rhizosphere (Fig. 3b) and
197 increased pore water concentrations of C and metals more than either glucose or acetic acid (Fig.
198 4a). Oxalic acid additions appear to increase microbial access to C in the pore water via this
199 mechanism.

200 To gain more detailed insights into the mechanisms of C mobilization, the chemical form of
201 pore water C and its association with inorganic constituents was determined using NanoSIMS and
202 STXM/NEXAFS imaging. NanoSIMS analysis of organic C in the pore water showed that only a small
203 fraction (< 2.5 %) was derived from ^{13}C-labeled exudates (Table S-9). This confirms that exudates
204 are rapidly removed from solution by microbial processing and/or adsorption to minerals [40], and

that dissolved compounds remaining in the pore water are predominantly derived from native soil C. STXM revealed that organic compounds isolated from the oxalic acid treatment showed only traces of Ca (Fe was below the detection limit), while organic C from the control treatment was associated with considerable amounts of Ca and Fe. Pore water C from the oxalic acid treatment also featured prominent resonances assigned to aromatic (1s-π* transitions of conjugated C=C) and carboxylic moieties (1-π* transition of COOH) in the corresponding NEXAFS spectra (Fig. 4c). In contrast, spectra of glucose, acetic acid, and control treatments did not indicate any aromatic C resonances – a pattern that was confirmed in forest soil subjected to the same treatments (Fig. S-5). Lignin-derived aromatic acids are strong metal chelators and are often associated with SRO minerals [41,42]. Crosslinking between these multivalent cations and carboxylic and phenolic groups facilitates aggregation and precipitation of organic compounds [43]. Oxalic acid, with its high ligand binding constant (Table 1), strips cations such as Fe and Ca from organic compounds in the pore water (Fig. 4b). In our experiment we observed enhanced solubility of organic compounds, supporting the hypothesis that oxalic acid removed the cations from MOCs. Based on our results, we conclude that oxalic acid addition increased pore water concentrations of aromatic and carboxylic C (Fig. 4c) associated with lignin-derived dimers (Fig. S-4). Low concentrations of oxalic acid released into the rhizosphere suffice to remobilize such compounds and enhance microbial access.

Root exudate-enhanced carbon accessibility: Implications for the terrestrial C cycle

As detailed above, we expected that an energetically more favorable root exudate such as glucose should cause a greater 'priming effect' than a less attractive one such as oxalic acid (Fig. 1a). However, the inverse was observed: by improving the accessibility of C previously protected in mineral-organic associations, oxalic acid induced a much stronger 'priming effect' than glucose and

acetic acid. Rather than via co-metabolism, organic ligands with metal-complexing abilities accelerate microbial mineralization of C in the rhizosphere via an indirect, multipart mechanism (Fig. 1b). Organic ligands released into the rhizosphere (i) mobilize mineral-bound C through complexation and dissolution of SRO phases and/or (ii) solubilize organic compounds through the removal of cross-linking metal cations from MOCs. Release from SRO or MOC phases promotes the accessibility of organic compounds to microbes. Increased microbial access subsequently (iii) stimulates microbial mineralization and shifts the community structure towards phyla adapted to soil environments with greater accessibility of C. Based on these results, we conclude that 'priming effects' is not a purely biotic phenomenon and should be viewed as the sum of direct biotic co-metabolic (Fig. 1a) and indirect C mobilization (Fig. 1b) mechanisms. We suggest that future investigations into the causes of 'priming effects' consider both mechanisms simultaneously and focus on quantifying their relative contributions in different soil ecosystems.

In our study, oxalic acid disrupted mineral-organic associations in both grassland and forest soils. This observation is consistent with root-induced weathering of protective mineral phases during periods of rapid root growth in arable [44] and forest soils [45], and highlights the general nature of the proposed mechanism. To estimate the importance of the proposed mechanism at the ecosystem-scale, we calculated the potential C loss that may be attributed to this mobilization mechanism in a forest ecosystem. The oxalic acid treatment resulted in an overall C loss of ~4% over our experimental test. If we assume that (i) the total amount of exudate carbon released into the soil in our experiments is comparable to that released over the course of an annual burst of root growth in times of high primary productivity [26] and (ii) organic acids comprise up to ~25% of the mixture of compounds exuded over that time frame [24] the annual C loss is estimated to be ~1% C yr^{-1}. By comparison, Richter et al. [46] found that soil C in deep mineral horizons, where C accessibility is likely low due to mineral-organic associations, is rapidly mineralized upon reforestation and expansion of the rooting zone. In that study, the average loss over four decades of reforestation was

254 approximately 1.08% C yr^{-1}, a rate strikingly close to the value in our experiment. Although simple,
255 our calculation highlights the potential impact of the proposed 'priming' mechanism on mineral
256 protected C at an ecosystem level.

257 Conceptual frameworks of soil organic matter stabilization have long considered C in
258 mineral-organic associations permanently inaccessible to microbes, and thus protected from loss
259 processes for millennia or longer [13,14,18]. But this paradigm is shifting, and many now recognize that
260 any natural organic compound can be decomposed when the required nutrients are available to the
261 decomposer community [21]. Here we demonstrate a climate-dependent 'priming' mechanism where
262 plant exudates counteract the strong protective effect of mineral-organic associations and facilitate
263 the loss of C from the soil system. This physiological capacity of plant roots to effectively remobilize
264 mineral-associated soil C will have to be factored into next-generation soil C cycling models [22,47] if
265 root exudation rates respond to global change as predicted. Elevated CO_2 concentrations may not
266 only stimulate exudation, they may also alter the composition of exudate compounds released into
267 soil [6,48] and increase metal mobilization in the rooting zone [49]. If shifts towards greater exudation of
268 reactive weathering agents such as oxalic acid [5] can be confirmed, determining how changing
269 exudation patterns impact mineral-protected C should be a high priority for future research.

270

Methods

Soils were chosen to represent two important biomes, forests and grasslands. Medium-textured silt-loam (*Typic Haploxeroll*) under cultivation with Triticum spp. (Hermiston Agricultural Research & Extension Center, Oregon, USA) and volcanic-ash clay (*Humic Dystrudept*) under old-growth Douglas-fir (H.J. Andrews Experimental Forest, Oregon, USA). At both sites, soil cores and mixed samples of surface horizons characterized by dense root networks were collected and stored at field moisture at 4˚C until further use (see Table S-1 for soil characteristics and handling).

Incubations were conducted in microcosm systems designed and fabricated to deliver a continuous supply of exudate solution through an artificial root into the soil (see SI for details). Soils were sieved (2 mm), pre-incubated at 75% field capacity for one week, and packed into the frame at field bulk density. The artificial roots were connected to a syringe pump equipped with a multi-syringe feeding system, which provided sterile exudate solutions containing glucose, acetic acid or oxalic acid as well as inorganic nutrients for osmoregulation (330 µM KCl, 70 µM KH_2PO_4 and 70 µM $MgSO_4$). Concentrations of each exudate solution were normalized on a C-basis and the pump rate was adjusted such that exudates were delivered at a rate of 15 µmol C cm^{-2} d^{-1} per microcosm at 1 ml d^{-1}. ^{13}C-labeled substrates (Cambridge Isotope Laboratories, Inc., Tewksbury, MA) were used to enrich exudate solutions in ^{13}C (final $\delta^{13}C$ = 8800 per mil). Incubations were carried out in the dark for 35 d, with temperature (25 ˚C) and relative humidity (75 %) controlled by an environmental chamber. Two replicate microcosms were assembled for each treatment.

O_2 concentration profiles were measured after the incubation period using Clark-type microsensors (OX-100, Unisense, Aarhus, Denmark). Microsensors had a 100-µm tip size, a stirring sensitivity of < 2 %, and a 90 % response time of < 1 s. Linear calibrations were performed in 0.1 M sodium ascorbate in 0.1 M NaOH (0% O_2 saturation) and air bubbled water (100% O_2 saturation) before and between measurements. The microsensor was mounted on a micromanipulator (MM33-

296 2, Unisense, Denmark) and connected to a picoamperemeter (PA-2000, Unisense, Denmark) to
297 collect six replicate measurements at distances of 0.5, 1, 5 and 15 mm from the root in each
298 microcosm (see SI for details).

299 After the incubation, microcosms were opened an anaerobic glove box and three zones on
300 both sides of the root (0-4, 5-12 and 13-50 mm from the root) were carefully sampled for metal and
301 DNA/RNA extractions, pH and total C measurements. Metal pools in each zone were determined
302 using a sequential extraction procedure consisting of (i) 0.1 M Na-pyrophosphate at pH 10 for
303 organically complexed pools, (ii) 1 M ammonium acetate at pH 3 for acid-soluble pools, and (iii) 0.2
304 M ammonium oxalate at pH 3 for short-range order phases. Duplicate extractions were performed
305 under anaerobic conditions in the dark. Elemental analysis of the supernatants was performed on a
306 Perkin Elmer SCIEX Elan DRC II Inductively Coupled Plasma Mass Spectrometer (ICP-MS). Total
307 RNA/DNA was extracted from 0.25 g soil of each zone using a MoBio PowerSoil RNA Isolation Kit in
308 combination with the PowerSoil DNA Elution Accessory Kit (MoBio Laboratories, Carlsbad, CA,
309 USA) following manufacturer's instructions. Dublicate extracts for each sample were prepared for
310 pyrosequencing (see SI for details).

311 Soil pore water was extracted from the root zone (0-4mm) using Whatman Centrex MF
312 Disposable Centrifugal Microfilter (Whatman Inc, Florham Park, NJ), adapting an existing low-
313 pressure centrifugal displacement technique [50]. In the glove box, a 2 g aliquot of moist soil was
314 transferred to the sample reservoir. Soil pore water was displaced and filtered through pre-rinsed
315 0.45 μm cellulose acetate membranes into the collection tube by centrifugation at 2000 × g for 60
316 min. Organic C concentrations in the pore water samples were determined by UV/vis (450 nm) and
317 the chemical composition was analyzed using laser desorption synchrotron ionization (LDSI). LDSI
318 was performed on a modified time-of-flight secondary ion mass spectrometer (TOF.SIMS V; IonTOF,
319 Germany) coupled to a synchrotron VUV light port at beamline 9.0.2 of the Advanced Light Source
320 (ALS) at the Lawrence Berkeley National Laboratory. For combined imaging analysis of pore water

C and associated metals, 1µL pore water aliquots were dried on Si_3N_4 windows (Silson Ltd, UK) in the glove box. STXM/NEXAFS spectromicoscopic analyses were performed at beamline 5.3.2.2 (250–600 eV) of the ALS [51]. $\delta^{13}C$ values of pore water C were acquired using high-resolution secondary ion mass spectrometry imaging performed on a NanoSIMS 50 (Cameca, Gennevilliers, France) at the Lawrence Livermore National Laboratory. Details on imaging analyses can be obtained in the SI. Reported results from statistical tests were obtained with OriginPro (OriginLab, Northampton, USA), including one-way ANOVA followed by post-hoc analysis using Tukey's hsd test (Fig. 2b, Fig. 3) and correlation analysis (Fig. 4a), with *p*-value of less than 0.05 indicating statistical significance.

Author contributions

M. Keiluweit performed microcosm setup, laboratory analyses, synchrotron analyses, data analysis and wrote the manuscript. J.J.B was responsible for DNA/RNA extractions and data processing. J.J.B and P.K.W. conducted NanoSIMS analyses. M. Kleber, J.P., P.K.W, and P.S.N. supervised the project. All authors discussed the results and contributed to the manuscript.

Acknowledgements

The authors thank A.L.D. Kilcoyne (ALS beamline 5.3.2.2), S.Y. Liu and M. Ahmed (ALS beamline 9.0.2) for their support. M. Keiluweit was supported by a Lawrence Scholar Fellowship awarded through Lawrence Livermore National Laboratory (LLNL). This work was performed under the auspices of the U.S. Department of Energy by LLNL under Contract DE-AC52-07NA27344. Funding was provided by LLNL LDRD "Microbes and Minerals: Imaging C Stabilization" and a US DOE Genomics Science program award SA-DOE-29318 to J.P.R. The work of P.S.N. is supported by LBNL award No. IC006762 as sub-award from LLNL and DOE-BER Sustainable Systems SFA. The Advanced Light Source is supported by the Director, Office of Science, Office of Basic Energy Sciences, of the U.S. DOE under Contract No. DE-AC02-05CH11231. LLNL-JRNL-644153

References

1. Högberg, P. *et al.* Large-scale forest girdling shows that current photosynthesis drives soil respiration. *Nature* **411,** 789–792 (2001).

2. Clemmensen, K. E. *et al.* Roots and associated fungi drive long-term carbon sequestration in boreal forest. *Science* **339,** 1615–1618 (2013).

3. Phillips, R. P., Finzi, A. C. & Bernhardt, E. S. Enhanced root exudation induces microbial feedbacks to N cycling in a pine forest under long-term CO2 fumigation. *Ecol. Lett.* **14,** 187–194 (2011).

4. Carney, K. M., Hungate, B. A., Drake, B. G. & Megonigal, J. P. Altered soil microbial community at elevated CO2 leads to loss of soil carbon. *Proc. Natl. Acad. Sci.* **104,** 4990–4995 (2007).

5. DeLucia, E. H., Callaway, R. M., Thomas, E. M. & Schlesinger, W. H. Mechanisms of phosphorus acquisition for ponderosa pine seedlings under high CO2 and temperature. *Ann. Bot.* **79,** 111–120 (1997).

6. Fransson, P. Elevated CO2 impacts ectomycorrhiza-mediated forest soil carbon flow: fungal biomass production, respiration and exudation. *Fungal Ecol.* **5,** 85–98 (2012).

7. Heimann, M. & Reichstein, M. Terrestrial ecosystem carbon dynamics and climate feedbacks. *Nature* **451,** 289–292 (2008).

8. Kuzyakov, Y., Friedel, J. K. & Stahr, K. Review of mechanisms and quantification of priming effects. *Soil Biol. Biochem.* **32,** 1485–1498 (2000).

9. Bianchi, T. S. The role of terrestrially derived organic carbon in the coastal ocean: A changing paradigm and the priming effect. *Proc. Natl. Acad. Sci. U. S. A.* **108,** 19473–19481 (2011).

10. Fontaine, S., Mariotti, A. & Abbadie, L. The priming effect of organic matter: a question of microbial competition? *Soil Biol. Biochem.* **35,** 837–843 (2003).

11. Horvath, R. S. Microbial co-metabolism and the degradation of organic compounds in nature. *Bacteriol. Rev.* **36,** 146–155 (1972).

12. Blagodatskaya, E. & Kuzyakov, Y. Mechanisms of real and apparent priming effects and their dependence on soil microbial biomass and community structure: critical review. *Biol. Fertil. Soils* **45,** 115–131 (2008).

13. Torn, M. S., Trumbore, S. E., Chadwick, O. A., Vitousek, P. M. & Hendricks, D. M. Mineral control of soil organic carbon storage and turnover. *Nature* **389,** 170–173 (1997).

14. Baisden, W. T., Amundson, R., Cook, A. C. & Brenner, D. L. Turnover and storage of C and N in five density fractions from California annual grassland surface soils. *Glob. Biogeochem. Cycles* **16,** 64–1–64–16 (2002).

15. Mikutta, R. *et al.* Biodegradation of forest floor organic matter bound to minerals via different binding mechanisms. *Geochim. Cosmochim. Acta* **71,** 2569–2590 (2007).

16. Chorover, J. & Amistadi, M. K. Reaction of forest floor organic matter at goethite, birnessite and smectite surfaces. *Geochim. Cosmochim. Acta* **65,** 95–109 (2001).

17. Conant, R. T. *et al.* Temperature and soil organic matter decomposition rates – synthesis of current knowledge and a way forward. *Glob. Change Biol.* **17,** 3392–3404 (2011).

18. Mikutta, R., Kleber, M., Torn, M. S. & Jahn, R. Stabilization of soil organic matter: association with minerals or chemical recalcitrance? *Biogeochemistry* **77,** 25–56 (2006).

19. Rasmussen, C., Southard, R. J. & Horwath, W. R. Soil Mineralogy Affects Conifer Forest Soil Carbon Source Utilization and Microbial Priming. *Soil Sci. Soc. Am. J.* **71,** 1141 (2007).

20. Kemmitt, S. J. *et al.* Mineralization of native soil organic matter is not regulated by the size, activity or composition of the soil microbial biomass—a new perspective. *Soil Biol. Biochem.* **40,** 61–73 (2008).

21. Schmidt, M. W. I. *et al.* Persistence of soil organic matter as an ecosystem property. *Nature* **478,** 49–56 (2011).

22. Tang, J. Y., Riley, W. J., Koven, C. D. & Subin, Z. M. CLM4-BeTR, a generic biogeochemical transport and reaction module for CLM4: model development, evaluation, and application. *Geosci. Model Dev.* **6,** 127–140 (2013).

23. Jones, D. L., Dennis, P. G. & van Hees, P. A. W. Organic acid behavior in soils-misconceptions and knowledge gaps. *Plant Soil* 31–41 (2003).

24. Neumann, G. & Roemheld, V. in *The Rhizosphere: Biochemistry and Organic Substances at the Soil-Plant Interface* (CRC Press, 2007).

25. Paterson, E. & Sim, A. Rhizodeposition and C-partitioning of Lolium perenne in axenic culture affected by nitrogen supply and defoliation. *Plant Soil* **216,** 155–164 (1999).

26. Phillips, R. P., Erlitz, Y., Bier, R. & Bernhardt, E. S. New approach for capturing soluble root exudates in forest soils. *Funct. Ecol.* **22,** 990–999 (2008).

27. Brant, J. B., Sulzman, E. W. & Myrold, D. D. Microbial community utilization of added carbon substrates in response to long-term carbon input manipulation. *Soil Biol. Biochem.* **38,** 2219–2232 (2006).

28. Frey, S. D., Lee, J., Melillo, J. M. & Six, J. The temperature response of soil microbial efficiency and its feedback to climate. *Nat. Clim. Change* **3,** 395–398 (2013).

29. Schneckenberger, K., Demin, D., Stahr, K. & Kuzyakov, Y. Microbial utilization and mineralization of [14C]glucose added in six orders of concentration to soil. *Soil Biol. Biochem.* **40,** 1981–1988 (2008).

30. Fierer, N., Bradford, M. A. & Jackson, R. B. Toward an ecological classification of soil bacteria. *Ecology* **88,** 1354–1364 (2007).

31. Eilers, K. G., Debenport, S., Anderson, S. & Fierer, N. Digging deeper to find unique microbial communities: The strong effect of depth on the structure of bacterial and archaeal communities in soil. *Soil Biol. Biochem.* **50,** 58–65 (2012).

32. Yan, F., Schubert, S. & Mengel, K. Soil pH increase due to biological decarboxylation of organic anions. *Soil Biol. Biochem.* **28,** 617–624 (1996).

33. McBride, M. B. *Environmental chemistry of soils*. (Oxford University Press, 1994).

34. Lovley, D. R. Dissimilatory Fe(III) and Mn(IV) reduction. *Microbiol. Rev.* **55,** 259–287 (1991).

35. Glinski, J., Stahr, K., Stepniewska, Z. & Brzezinska, M. Changes of Redox and pH Conditions in a Flooded Soil Amended with Glucose and Nitrate under Laboratory Conditions. *J. Plant Nutr. Soil Sci.* **155,** 13–17 (1992).

36. Hamer, U. & Marschner, B. Priming effects in different soil types induced by fructose, alanine, oxalic acid and catechol additions. *Soil Biol. Biochem.* **37,** 445–454 (2005).

37. Falchini, L., Naumova, N., Kuikman, P. J., Bloem, J. & Nannipieri, P. CO2 evolution and denaturing gradient gel electrophoresis profiles of bacterial communities in soil following addition of low molecular weight substrates to simulate root exudation. *Soil Biol. Biochem.* **35,** 775–782 (2003).

38. Liu, S. Y. *et al.* Synchrotron-based mass spectrometry to investigate the molecular properties of mineral–organic associations. *Anal. Chem.* **85,** 6100–6106 (2013).

39. Hanley, L. & Zimmermann, R. Light and molecular Ions: the emergence of vacuum UV single-photon ionization in MS. *Anal. Chem.* **81,** 4174–4182 (2009).

40. Fischer, H., Ingwersen, J. & Kuzyakov, Y. Microbial uptake of low-molecular-weight organic substances out-competes sorption in soil. *Eur. J. Soil Sci.* **61,** 504–513 (2010).

41. Mikutta, R. *et al.* Biogeochemistry of mineral–organic associations across a long-term mineralogical soil gradient (0.3–4100kyr), Hawaiian Islands. *Geochim. Cosmochim. Acta* **73,** 2034–2060 (2009).

42. Kramer, M. G., Sanderman, J., Chadwick, O. A., Chorover, J. & Vitousek, P. M. Long-term carbon storage through retention of dissolved aromatic acids by reactive particles in soil. *Glob. Change Biol.* **18,** 2594–2605 (2012).

43. Kunhi Mouvenchery, Y., Kučerík, J., Diehl, D. & Schaumann, G. E. Cation-mediated cross-linking in natural organic matter: a review. *Rev. Environ. Sci. Biotechnol.* **11,** 41–54 (2011).

44. Fischer, W. R., Flessa, H. & Schaller, G. pH values and redox potentials in microsites of the rhizosphere. *Z. Für Pflanzenernähr. Bodenkd.* **152,** 191–195 (1989).

45. Collignon, C., Ranger, J. & Turpault, M. P. Seasonal dynamics of Al- and Fe-bearing secondary minerals in an acid forest soil: influence of Norway spruce roots (Picea abies (L.) Karst.). *Eur. J. Soil Sci.* **63,** 592–602 (2012).

46. Richter, D. D., Markewitz, D., Trumbore, S. E. & Wells, C. G. Rapid accumulation and turnover of soil carbon in a re-establishing forest. *Nature* **400,** 56–58 (1999).

47. Wieder, W. R., Grandy, A. S., Kallenbach, C. M. & Bonan, G. B. Integrating microbial physiology and physio-chemical principles in soils with the Microbial-Mineral Carbon Stabilization (MIMICS) model. *Biogeosciences* **11,** 3899–3917 (2014).

48. Hodge, A. *et al.* Characterisation and microbial utilisation of exudate material from the rhizosphere of Lolium perenne grown under CO2 enrichment. *Soil Biol. Biochem.* **30,** 1033–1043 (1998).

49. Cheng, L. *et al.* Atmospheric CO_2 enrichment facilitates cation release from soil. *Ecol. Lett.* **13,** 284–291 (2010).

50. Pérez, D. V., de Campos, R. C. & Novaes, H. B. Soil solution charge balance for defining the speed and time of centrifugation of two Brazilian soils. *Commun. Soil Sci. Plant Anal.* **33,** 2021–2036 (2002).

51. Kilcoyne, A. L. D. *et al.* Interferometer-controlled scanning transmission X-ray microscopes at the Advanced Light Source. *J. Synchrotron Radiat.* **10,** 125–136 (2003).

52. Smith, R. M. & Martell, A. E. Critical stability constants, enthalpies and entropies for the formation of metal complexes of aminopolycarboxylic acids and carboxylic acids. *Sci. Total Environ.* **64,** 125–147 (1987).

53. Højberg, O. & Sørensen, J. Microgradients of microbial oxygen consumption in a barley rhizosphere model system. *Appl. Environ. Microbiol.* **59,** 431–437 (1993).

Table 1: a) Exudate properties and their b) predicted and c) measured effect on microbial carbon-use efficiency (CUE) and biochemical oxygen demand (BOD)

	Properties		Glucose	Acetic acid	Oxalic acid
a)	Acidity (pK_a)		n.a.	4.76	1.25 and 4.14
	Complexation of Fe^{3+} (log$K$) ¶		n.a.	3.5	8.2
b)	CUE# (ratio)		0.4-0.7	0.4-0.6	0.05-0.25
	Stoichiometric BOD (mol O_2 mol^{-1} C)		1	1	0.25
	Expected BOD§ (mol O_2 mol^{-1} C)		0.3-0.6	0.4-0.6	0.23-0.30
c)	Expected BOD&		1.0-2.0	1.3-2.0	0.7-1.0
	Measured respiration rates&	silt-loam	1.0 ± 0.3	0.5 ± 0.0	1.5 ± 0.0
		clay	1.0 ± 0.4	1.0 ± 0.5	2.4 ± 0.2

¶ formation constants (log$K$) defined by the equilibrium constant K = {ML}/({M}+{L}) where M is Fe^{3+} and L is either glucose, acetic acid or oxalic acid [52].

* measure of chemical energy of a substrate per unit mole of C.

reported microbial CUEs in soil incubations [27–29] expressed as the amount of C assimilated in new biomass relative to the amount of C used in cellular respiration.

§ range of expected BOD in soils calculated as (1 – CUE) × stoichiometric BOD.

& expected BOD values and measured O_2 respiration rates given relative to those for glucose.

470

Figure captions

Figure 1: Proposed mechanisms for the exudate-induced acceleration of the microbial mineralization of native carbon ('priming effects') in the rhizosphere. (a) The traditional view is that reduced exudate compounds (e.g., simple sugars) stimulate microbial growth and activity via co-metabolism, and so increase the overall physiological potential of the decomposer community for carbon mineralization. Other factors such as the increased microbial demand for nitrogen or successional shifts in the community structure may also contribute to increased mineralization rates [8,12]. (b) The alternative mechanism proposed here takes into account that large quantities of soil C are inaccessible to microbes due to associations with mineral phases. Root exudates that can act as ligands (e.g., organic acids) effectively liberate C through complexation and dissolution reactions with protective mineral phases, thereby promoting its accessibility to microbes and accelerating its loss from the system through microbial mineralization.

Figure 2: Exudate effects on artificial rhizosphere soil. (a) Photograph of the rhizosphere effect caused by oxalic acid addition and the control for comparison. White arrows indicate positions of the artificial root providing exudate solutions. (b) O_2 concentrations as a function of distance to the root for the different exudate treatments. Points represent mean ± standard error of the mean (n = 2). Asterisks denote locations with mean O_2 concentrations significantly lower than the control (one-way ANOVA. Tukey's *ad-hoc* HSD test, $p < 0.05$). Solid lines represent model fits used to calculate microbial respiration based on Fick's first law of diffusion [53]. The inset shows volume-specific respiration rates in the rhizosphere for each exudate treatment. See SI for details on fitting parameters and rate calculations.

Figure 3: Exudate-induced effects on (a) total soil C and (b) protective mineral phases. Total C as well as Fe and Al bound in metal-organic complexes (MOCs) and short-range order (SRO) phases are presented as a function of distance to the root. Treatment effects were calculated as the percentage difference between concentrations in treatment and control samples for each distance. Positive values indicate a treatment-induced pool increase, while negative values indicate a pool decrease. Asterisks denote pool sizes significantly different from the control (One-way ANOVA, Tukey's *ad-hoc* HSD, $p < 0.05$). Values are shown as means ± standard error (n = 2). Data shown for silt-loam grassland soils only. Changes in metal pools of the clay-rich forest soil can be found in the SI (Fig. S-6).

Figure 4: Exudate effect on metal-organic associations in the pore water. (a) C mobilization into the pore water in relation to dissolved Fe concentrations. (b) Ca and Fe associated with dissolved organic C collected from control and oxalic acid treatments. Maps are generated as difference maps of two image scans collected above and below the respective absorption edge energies. (c) Carbon K-edge NEXAFS spectra of pore water C. Spectra of discrete regions of interest are shown as dotted lines, with the blue lines and shaded areas representing mean and standard deviation, respectively. The number of regions analyzed was 8 for glucose, 9 for acetic acid, 10 for oxalic acid, and 9 for the control. Data shown for silt-loam grassland soils only. Carbon NEXAFS spectra for clay-rich forest soil (Fig. S-5) and details on the STXM maps can be found in the SI.

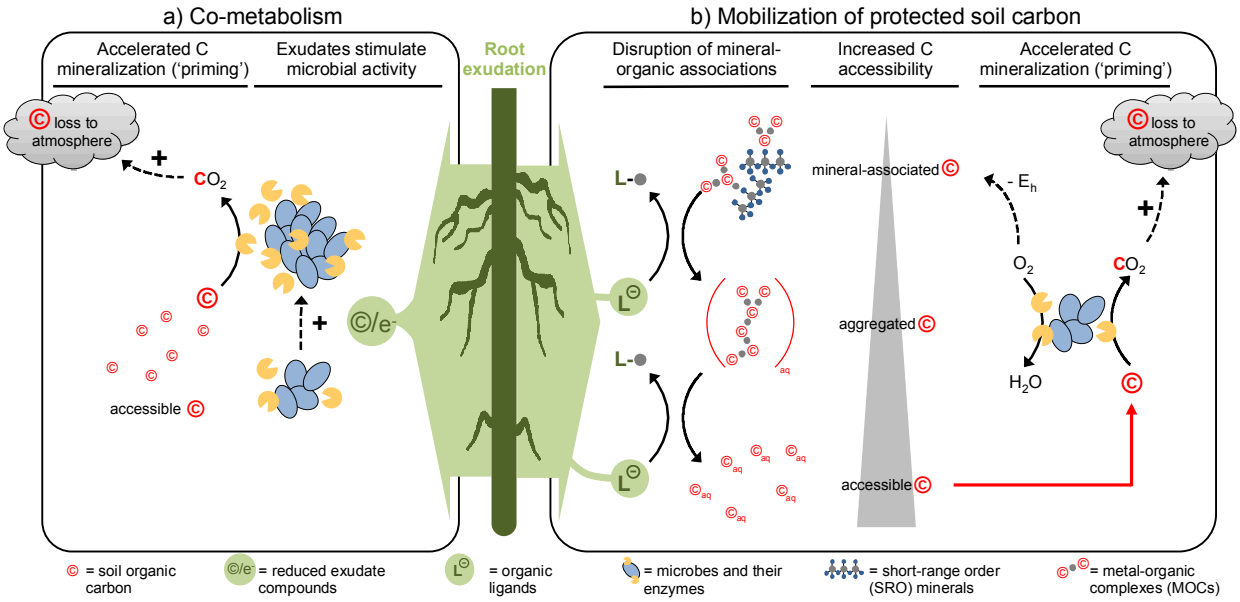

516

517 **Figure 1**

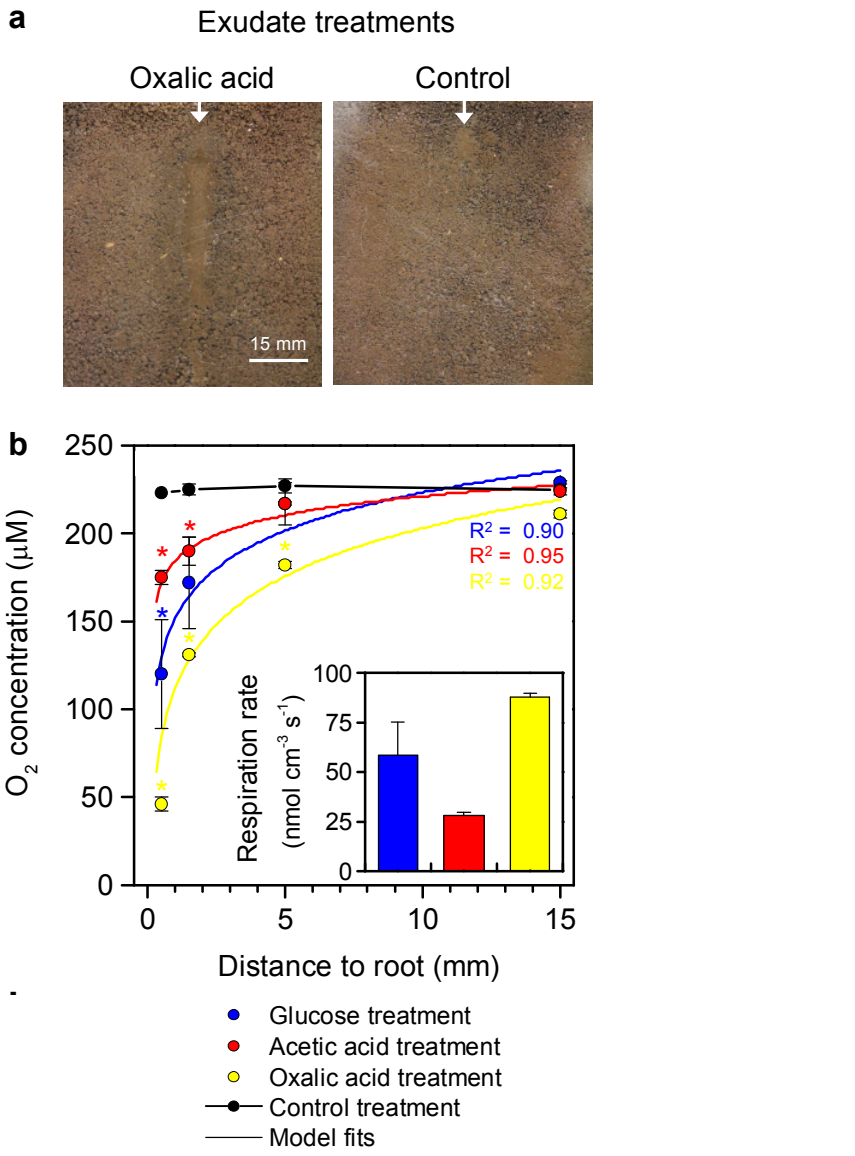

518

519 **Figure 2**

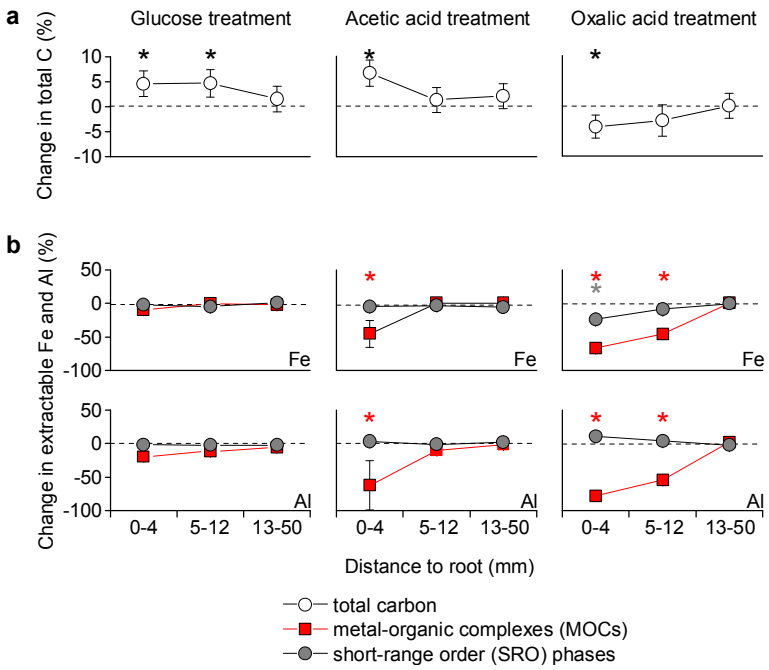

520

521 **Figure 3**

522

523

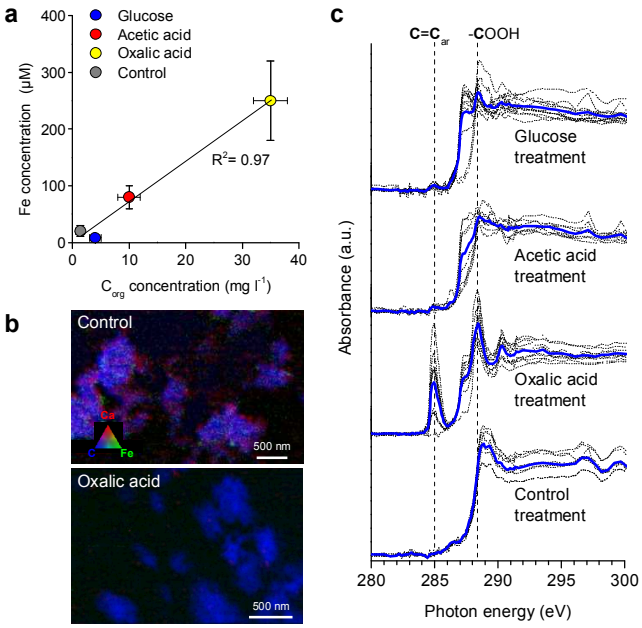

524

525 **Figure 4**

526